A Passive System Approach to Increase the Energy Efficiency in Walk Movements Based in a Realistic Simulation Environment

José L. Lima, José A. Gonçalves, Paulo G. Costa and A. Paulo Moreira

***Abstract*— This paper presents a passive system that increases the walk energy efficiency of a Humanoid robot. A passive system is applied to the simulated robot allowing the energy consumption to be reduced. The optimal parameters for the passive system depend on the joint and gait trajectories. Final results prove the benefits of the presented system apply. It was optimized thanks to a realistic simulator where the humanoid robot was modeled. The model was validated against a real robot.**

I. INTRODUCTION

Newfound research in biped robots has resulted in a variety of prototypes that resemble their biological counterparts. There are several advantages associated with legged robots: they can move in rugged terrains, they have the ability to choose optional landing points, and two legged robots are more suitable to move in a human environment. Consequently, research on biped robots is very active [1]. As humanoid robots are powered by on-board batteries, its autonomy depends on the energy consumption. The trajectory controller can also be optimized having in mind the energy consumption minimization [2] and walking gate optimization [3]. This paper addresses a passive system, that coupled to the humanoid robot joints, allows to save energy. The passive system optimal characteristics depend on each joint desired trajectory. These characteristics can be found by an optimization method. For this purpose, a realistic model for the simulator (SimTwo [4]) was developed. There are several simulators with humanoid simulation capability, like Simspark, Webots, MURoSimF, Microsoft Robotics Studio and YARP: Yet Another Robot Platform [5]. SimTwo, as a generic simulator, allows to simulate different types of robots and allows the access to the low level behaviour, such as dynamical model, friction model and servomotor model in a way that can be mapped to the real robot, with a minimal overhead. This simulator deals with robot dynamics and how it reacts for several controller strategies and styles. It is not an easy task to develop such model for the robot due to the inherent complexity of building realistic models for its physics, its sensors and actuators and their interaction with the world [6]. The paper is organized as follows: Initially, the real robot (which is the system that was modeled in the simulator) and its control architecture are described. Then, section 3 presents the developed simulator. The servo and friction models are presented. Further, section 4 presents the energy efficiency increase based in a passive system approach where optimal parameters are found. Finally, section 5 rounds up with conclusions and future work.

José L. Lima and José A. Gonçalves are with Polytechnic Institute of Bragança, {jllima,goncalves}@ipb.pt

Paulo G. Costa and A. Paulo Moreira are with the Faculty of Engineering of University of Porto, {paco,amoreira}@fe.up.pt

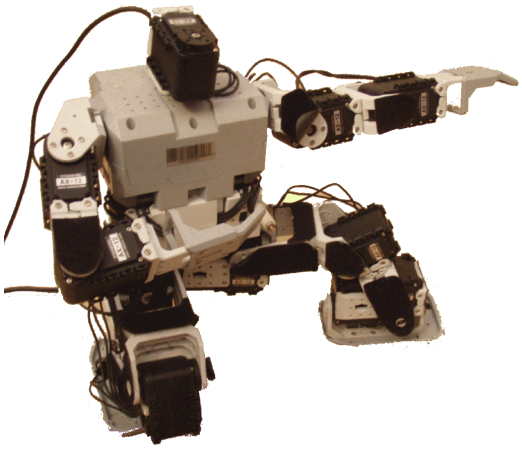

Fig. 1. Real humanoid robot

II. REAL HUMANOID

There are several humanoid robots kits available. The commercially available Bioloid robot kit, from Robotis, served as the basis for the humanoid robot and the proposed biped robot is shown in Fig. 1.

The servo motors are connected to the central processing unit (CM-5), based on the ATMega128 microcontroller, through a serial 1Mbps network. The original firmware presented in the CM-5 can be replaced in order to develop a personalized control application. Its manufacturer provides the source code making it easier to develop a new firmware. Next subsections present the physical robot in which the developed humanoid simulator was based.

A. Main Architecture

The presented humanoid robot is driven by 19 servo motors (AX-12): six per leg, three in each arm and one in the head. Three orthogonal servos set up the 3DOF (degree of freedom) hip joint. Two orthogonal servos form the 2DOF ankle joint. One servo drives the head (a vision camera holder). The shoulder is based on two orthogonal servos allowing a 2DOF joint and elbow has one servo allowing 1DOF. The total weight of the robot (without camera and onboard computer) is about 2 kg and its height is 38 cm.

B. Control Architecture

Multiple layers that run on different time scales contain behaviours of different complexity. The layer map is presented in Fig. 2.

The lowest level of this hierarchy, the control loop within the Dynamixel actuators (AX-12), has been implemented by Robotis. The servomotor is an embedded system, based on a ATMega8 microcontroller, that has an identifier ID

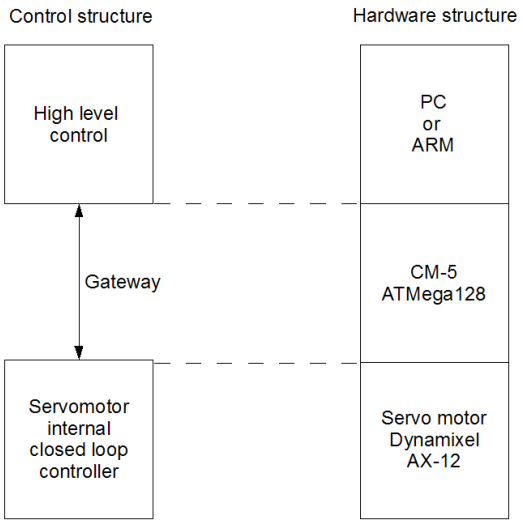

Fig. 2. Architecture levels of real robot

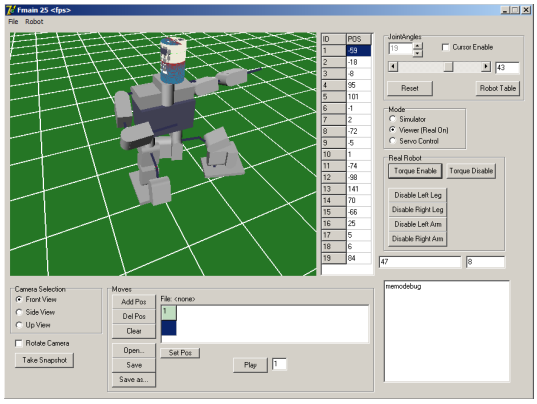

Fig. 3. Control application

and receives commands from the bus shared for all servomotors. It is mainly composed by a DC motor and a PWM driver. Each servo is able to be programmed with not only the goal position, the moving speed, the maximum torque, the temperature and voltage limits but also with the control parameters. These limitations are presented in the simulator for a faithful representation. At the next layer, the CM-5 module interface, allows for data interchange. It receives messages from the upper layer and translates them to the servos bus. Answers from servos are also translated and sent back to the upper layer. Fig. 3 shows the developed high level application that allows to control the real humanoid robot. This application is independent from the simulator.

III. Simulation Model

Design behaviour without real hardware is possible due to a physics-based simulator implementation. The physics engine is the key to make simulation useful in terms of high performance robot control [6]. The dynamic behaviour of robot (or multiple robots) is computed by the ODE Open Dynamics Engine, a free library for simulating rigid body dynamics.

A. Simulator Architecture

The simulator architecture is based on the real humanoid robot. The simulated body masses and dimensions are the same as the real one. The communication architecture in the real robot brings some limitations to control loop such as lag time. The developed simulator implements these properties and the same architecture levels of the real robot are implemented in the simulator. The simulation step is 500 μs and the controller loop period is done at 40 ms. At the lowest level, the servo motor model includes the control loop, just like the real servomotors. At the highest level, some predefined joint states are created based on several methods presented on literature: [7], [8] and [9]. It is also implemented, at the middle level, an optimized trajectory controller that allows to minimize acceleration, speed or energy consumption [2].

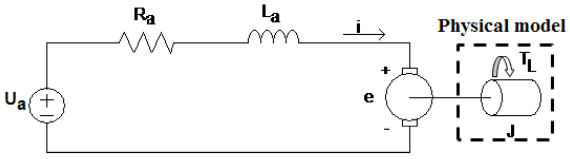

Fig. 4. Servomotor model electric scheme

B. Servomotor Model

The servomotor can be resumed to a DC motor model, presented in Fig. 4 where U_a is the converter output, R_a is the equivalent resistor, L_a is the equivalent inductance and e is the back emf voltage as expressed by (1).

The parameters of the motor can be measured directly or through some experiments: R_a is 8 Ω, L_a is 5 mH and K_s is 0.006705 $V.s/rad$. The motor can supply a T_L torque and load has a J moment of inertia that will be computed by the physical model ODE. Current i_a can be correlated with developed torque T_D through (2) and the back emf voltage can be correlated with angular speed through (3), where K_s is a motor parameter [10].

$$U_a = e + R_a i_a + L_a \frac{\partial i_a}{\partial t} \tag{1}$$

$$T_D(t) = K_s i(t) \tag{2}$$

$$e(t) = K_s \omega(t) \tag{3}$$

In fact, the real developed torque (useful) that will be applied to the load (T_L) is the developed torque subtracted by the friction torque, presented in next subsection.

C. Friction Model

Friction exists in the simulator in two cases: The foot ground interaction and the joint connectivity. The first one, is adjusted so that displacement is the same as reality. The joint friction model becomes from two ways: the static and viscous friction. The first one can be modelled as the sign function (with F_c constant) and the second one can be modelled as a linear function with slope B_v. The final friction model is shown in Fig. 5.

The F_c and B_v constants are found using simulator scanning several possible values minimizing the error with the real system during an arm fall from 90 to 0

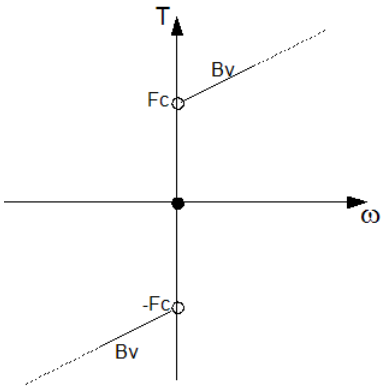

Fig. 5. Friction model: static and viscous

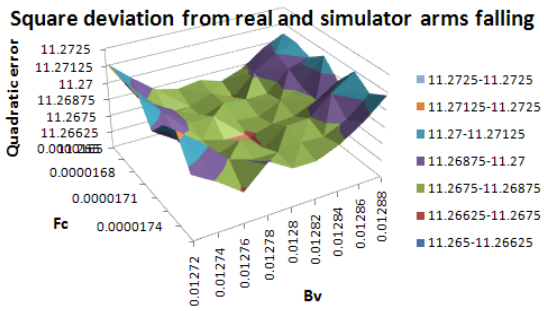

Fig. 6. Deviation from real and simulator frictions constants

$degrees$. Fig. 6 shows the surface of error between real and simulator robots.

As result, B_v=0.01278 $N.m.s/rad$ and F_c=0.0000171 $N.m$ shows the best values. These constants allows simulator to follow reality very close as presented in Fig. 7 where an arm falls from 45, 90 and 135 degrees for both robots.

D. Simulator Validation

A way to validate the humanoid simulation model is to apply the same control signal to both robots and to analyze the behavior. Predefined trajectory states, that allow robot to walk, are based on the Zero Moment Point (ZMP) method and are well described in literature [7] [8] [11]. Fig. 8 shows the sequence during walk movements for both robots (real at left and simulator at right).

It is possible to observe that both robots exhibit a very similar behavior. Furthermore, information from servomotors can be acquired with the developed control

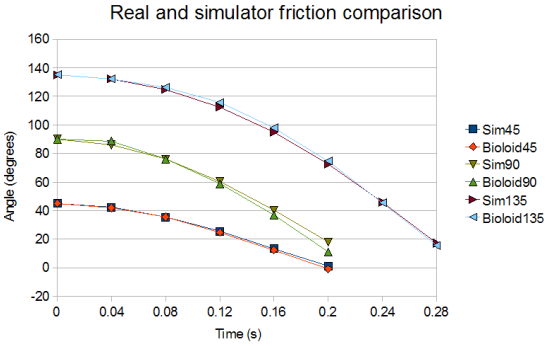

Fig. 7. Real and simulator friction comparison

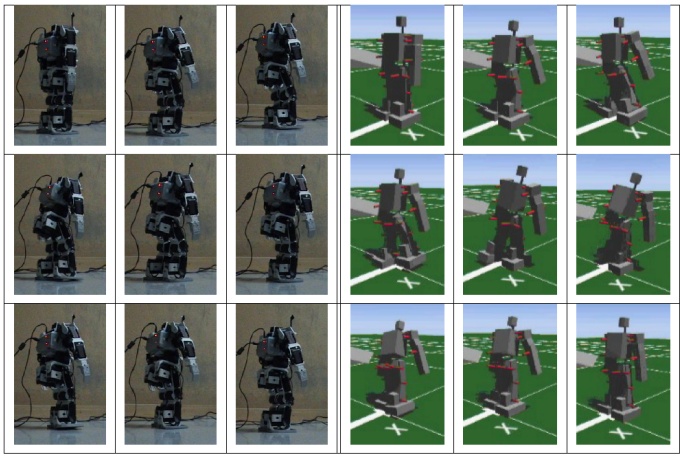

Fig. 8. Real and simulator robots walking with the same predefined gaits

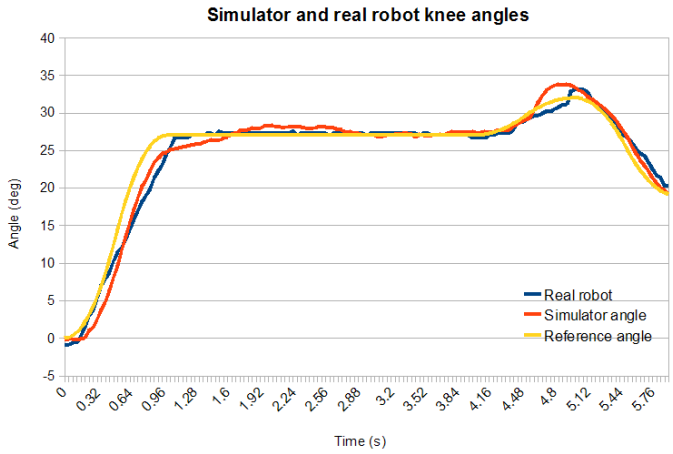

Fig. 9. Simulator and real humanoid robot knee behaviour

application and then compared with the simulator. Fig. 9 shows the knee angle of simulator and real robot for the same reference that seems to be very close. Finally, previous work presents energy consumption comparison for simulator and the real one on get up movements [12].

E. Humanoid Simplified Model

In order to get lower numerical errors during simulations, the total number of connected joints should be reduced. That problem comes from the way that the joint constraints are implemented by the ODE. For the simulation, it can be used a simplified model, presented in Fig. 10, with the same dimensions and weights of the humanoid robot, as only legs are important to this case and other joints are static. So, arms and rotational joints are dropped, resulting in three basic joints: ankle, knee and hip for each leg. The trunk is composed by an oscillating body that maintains the equilibrium during walk movements. Its length depends on the oscillating angle. This model has lower numerical errors in the simulator, as it has fewer articulations.

The presented simplified model will be used in next section.

IV. Energy Efficiency Increase

Having in mind the potential energy (E_p), presented in (4), where m is the body mass, g is the gravitational

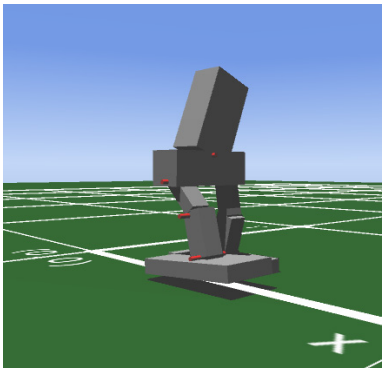

Fig. 10. Simplified model of humanoid robot

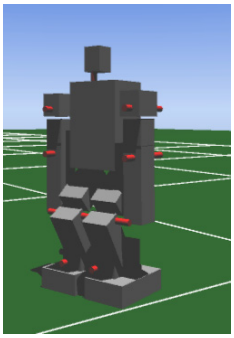

Fig. 11. Humanoid simulator in low level posture

acceleration and h is the height of the body, it can be shown that when the body goes down, it loses its energy that cannot be recovered.

$$E_p = mgh \tag{4}$$

Besides, the energy consumed to keep the robot in a low level posture (usually used during a walk movement as presented in Fig. 11) cannot be neglected due to the R_a resistor from the servomotor model (Joule effect). The power dissipated P_D, during a static pose in R_a resistor can be found in (5) where T_h the holding torque to keep the joint in the desired angle and the T_{ae} is the static friction force. This way, while robot keeps its low posture and when it rises, the consumed energy is provided only from batteries. While moving, the power consumption can be estimated in the simulator through voltage and current product and energy consumption for a movement can be computed through the power integral. This energy consumption can be used to find the optimal characteristics.

$$P_D = R_a \frac{(T_h - T_{ae})^2}{K_s^2} \tag{5}$$

Next section presents a solution that allows to decrease the power consumption, based on a passive method that increases the energy efficiency. The presented results, that validate the proposed approach, are extracted from a walk movement and based in the estimated energy consumption minimization.

A. Proposed Method

To store the potential energy and assist during low postures, an elastic element can be used. When the robot posture rises, the elastic element releases the stored energy. This elastic element is composed by a spring and its force can be calculated through $Hooke$ law, as presented in (6), where T_m is the torque, α_m is the torsion angle and k is a spring characteristic. The best spring type is a spiral one due to the nature of the system (torsion). The zero position can be changed and an $offset$ appears.

$$T_m = k(\alpha_m - offset) \tag{6}$$

In order to analyze the energy consumption during movements, the integral of the power must be computed. The power can be calculated by the voltage and current product. The current should only be used when its signal is the same as the voltage, as the power supply and the PWM driver are not regenerative.

B. Optimal Characteristics Computation

In order to compute the optimal characteristics for each spring (added to each joint), the walk movement was implemented for the robot and energy consumption was estimated for each joint. As the spring characteristics to be found, several values for k and $offset$ are implemented and the final energy consumption function allows to find the optimal characteristics at the minimum point. The inter-dependences between parameters can be despised whereas the joints controller keep the desired angle.

Figures presented in table I displays a graphic simulation snapshots of the walking robot model. Once walk movements are not symmetric, energy consumption can be different in legs.

To know the functions surfaces, the k and $offset$ scanning graphics for the minimum energy consumption are presented in figures 12, 13, 14, 15, 16, 17 and 18 for left and right ankles, left and right knees, left and right hips and equilibrium trunk.

Table II presents, in a short way, the optimal characteristics results for each one of the seven joints presented in the simplified robot.

C. Results

As result, it is possible to remark that the use of optimal spring's characteristics in the joints allows to decrease the energy consumption. In this case, 18.8 % of the energy can be saved as presented in table III.

Fig. 19 presents a comparison bar graphic for the energy consumption for each joint, with and without spring.

TABLE I

SIMPLIFIED MODEL COMPLETE WALKING SNAPSHOTS

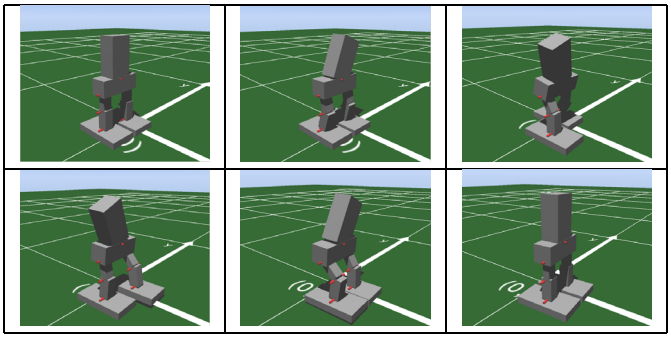

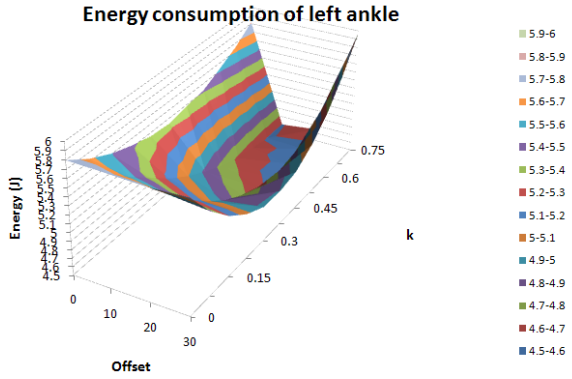

Fig. 12. Energy consumption of left ankle

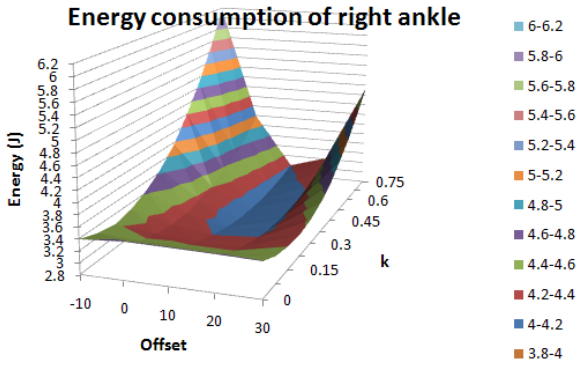

Fig. 13. Energy consumption of right ankle

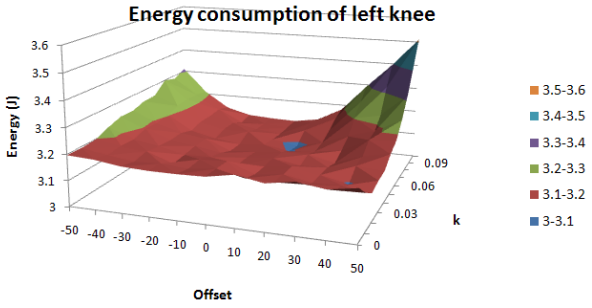

Fig. 14. Energy consumption of left knee

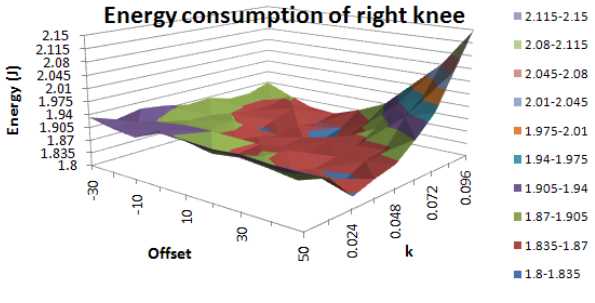

Fig. 15. Energy consumption of right knee

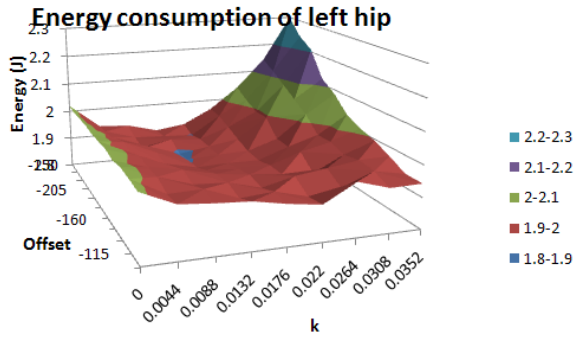

Fig. 16. Energy consumption of left hip

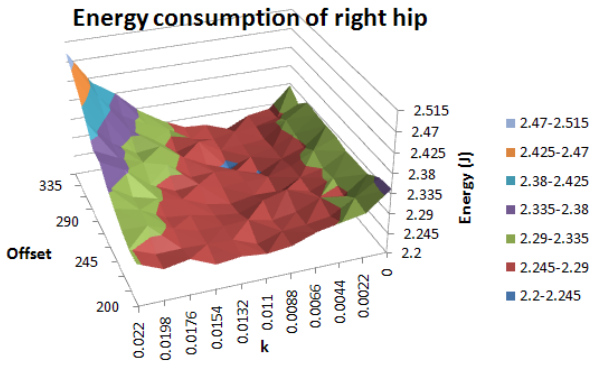

Fig. 17. Energy consumption of right hip

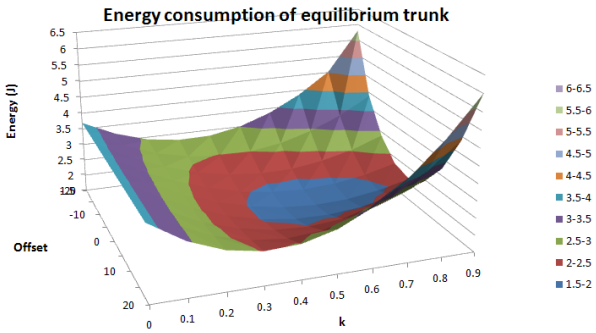

Fig. 18. Energy consumption of equilibrium trunk

TABLE II
K AND $offset$ OPTIMAL VALUES

Joint	k $(N.m^{-1})$	$offset$ (deg)
Left ankle	0.525	20
Right ankle	0.525	10
Left knee	0.07	10
Right knee	0.072	10
Left hip	0.0131	-205
Right hip	0.0088	305
Eq. trunk	0.6	0

TABLE III

ENERGY CONSUMPTION IN A WALK MOVEMENT PERIOD

Joint	En w/o spr (J)	En w/ spr (J)	Gain (%)
Left ankle	5.79	4.55	21.5
Right ankle	3.42	2.84	17.2
Left knee	3.18	3.09	3.0
Right knee	1.93	1.82	5.8
Left hip	2.02	1.89	6.2
Right hip	2.33	2.24	3.9
Eq. trunk	3.70	1.74	53.08
Total En.	22.38	18.16	18.8

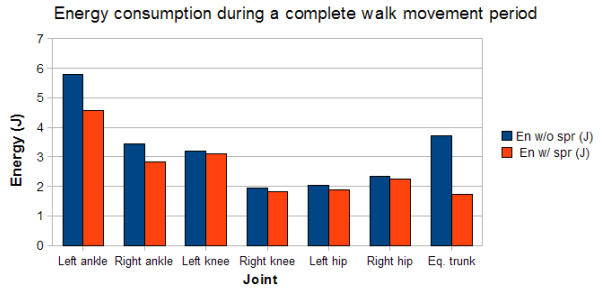

Fig. 19. Energy consumption comparison during a walk movement period

The equilibrium trunk joint is the most perceptible example. Excluding this joint, there is still a 12 % of energy that can be saved with springs. This shows that the use of the suggested springs in humanoid robotics articulations can increase the robot autonomy.

V. CONCLUSIONS

In the presented work, a simulator model of a humanoid platform was developed. Servomotor, friction and dynamic models were developed and validated. The passive system that increases energy efficiency was presented and the energy saving results were shown. The presented approach allows reducing energy consumption in 19 %. The initial results are found to be satisfactory, and improvements are currently underway to explore and enhance the capabilities of the proposed method. Henceforth, its adaptation to a real humanoid joint is the final implementation step.

REFERENCES

[1] Suzuki, T. and Ohnishi, K., Trajectory Planning of Biped Robot with Two Kinds of Inverted Pendulums, Proceedings of 12th International Power Electronics and Motion Control Conference, pp. 396-401, Portoroz, Slovenia (2006).

[2] Lima, J., Gonçalves, J., Costa, P. and Moreira, A., Humanoid robot simulation with a joint trajectory optimized controller, In Proceedings of 13th IEEE International Conference on Emerging Technologies and Factory Automation, Hamburg, German (2008).

[3] Tang, Z., Zhou, C. and Sun, Z. Humanoid Walking Gait Optimization Using GA-Based Neural Network, Advances in Natural Computation, pp. 252-261, Springer Berlin/Heidelberg, Changsha, China (2005).

[4] http://www.fe.up.pt/˜paco/wiki/

[5] Wang, X., Lu, T. and Zhang, P., YARP: Yet Another Robot Platform, International Journal of Advanced Robotic Systems, Vol. 3, No. 1, pp. 043-048 (2006).

[6] Browning, B. and Tryzelaar, E., UberSim: A Realistic Simulation Engine for RobotSoccer, Proceedings of Autonomous Agents and Multi-Agent Systems, Melbourne, Australia (2003).

[7] Kajita, S., Morisawa, M., Harada, K., Kaneko, K., Kanehiro, F., Fujiwara, K. and Hirukawa, H., Biped walking pattern generator allowing auxiliary ZMP control, Proceedings of IEEE/RSJ International Conference on Intelligent Robots and Systems, pp. 2994-2999, Beijing, China (2006).

[8] Zhang, L., Zhou, C. and Xiong, R., A lie group formulation for realtime zmp detection using force/torque sensor, In Proceedings of the 11th International Conference on Climbing and Walking Robots and the Support Technologies for Mobile Machines, pp. 1250-1257, Coimbra, Portugal (2008).

[9] Wang, X., Lu, T. and Zhang, P., State Generation Method for Humanoid Motion Planning Based on Genetic Algorithm, Journal of Humanoids, Vol. 1, No. 1, pp. 17-24, (2008).

[10] Bishop, R., The Mechatronics Handbook, CRC Press, New York (2002).

[11] Meghdari, A., Sohrabpour, S., Naderi, D., Tamaddoni, S., Jafari, F. and Salarieh, H., A Novel Method of Gait Synthesis for Bipedal Fast Locomotion, Journal of Intelligent and Robotic Systems, Volume 53, Number 2, pp. 99-202, Springer Netherlands (2008).

[12] Lima, J., Gonçalves, J., Costa, P. and Moreira, A., Realistic Behaviour Simulation of a Humanoid Robot, 8th Conference on Autonomous Robot Systems and Competitions, Aveiro, Portugal (2008).